We are IntechOpen,
the world's leading publisher of
Open Access books
Built by scientists, for scientists

4,800
Open access books available

122,000
International authors and editors

135M
Downloads

Our authors are among the

154
Countries delivered to

TOP 1%
most cited scientists

12.2%
Contributors from top 500 universities

CLARIVATE ANALYTICS
BOOK CITATION INDEX
INDEXED

WEB OF SCIENCE™

Selection of our books indexed in the Book Citation Index
in Web of Science™ Core Collection (BKCI)

Interested in publishing with us?
Contact book.department@intechopen.com

Numbers displayed above are based on latest data collected.
For more information visit www.intechopen.com

Chapter

Actively Controlled Journal Bearings for Machine Tools

Jiří Tůma, Jiří Šimek, Miroslav Mahdal, Jaromír Škuta, Renata Wagnerová and Stanislav Žiaran

Abstract

The advantage of journal hydrodynamic bearings is high radial load capacity and operation at high speeds. The disadvantage is the excitation of vibrations, called an oil whirl, after crossing a certain threshold of the rotational speed which depends on the radial bearing clearance, the viscosity of lubricating oil, and the rotor mass. A passive way of how to suppress vibrations consists of adjusting the shape of the bearing bushing. Vibrations can be suppressed using the system of active vibration damping with piezoactuators to move the bearing bushing in two directions. The displacement of the bearing bushing is actuated by two piezoactuators, which respond to the position of the bearing journal relative to the bearing housing. Two stacked linear piezoactuators are used to actuate the location of the bearing bushing. A pair of capacitive sensors senses the position of the journal or shaft. The system of the actively controlled journal bearings is the first functional prototype in the known up to now. It works with a cylindrical bushing which does not require special technology of manufacturing and assembly. This new bearing enables not only to damp vibrations but also serves to maintain the desired bearing journal position with an accuracy of micrometers.

Keywords: journal bearings, active vibration control, piezoactuators, oil whirl

1. Introduction

The reasons for the interest in actively controlled journal bearings (alternatively called sleeve bearings or plain bearings for radial load) lie in demand for the introduction of high-speed cutting or machining as a technology for the future. Increasing the machining speed was required to get beyond the limits of the interval, where unwanted temperature increases. Some researchers define high-speed machining as machining whereby conventional cutting speeds are exceeded by a factor of 5–10. Increased machining speed has advantages. The ability to benefit the advantages of high-speed cutting in steel, cast iron, and nickel-based alloys can be obtained with spindle speeds in the range of 8k to 12k rpm. High-speed cutting of nonferrous materials such as brass, aluminum, and engineered plastics demands a significantly higher rpm capability. For these materials, we must focus on milling equipment capable of operating at high-speed spindle speeds of 25k to 50k rpm or more. High-speed machining can also include grinding and turning.

Let us now notice the machine tool spindles. Roller bearings support these spindles. Prestressed ball or tapered roller bearings are used to eliminate play. This chapter focuses on plain radial bearings, namely, hydrodynamic bearings. Plain bearings of this type require a clearance for their function, which is selected in the range of 0.1–0.3% of the journal diameter.

Journal hydrodynamic bearings are a standard solution to support rotors. Their advantage is a possibility to carry the high radial load and to operate at high rotational speeds. The disadvantage of the journal bearings is the excitation of unwanted rotor vibrations by whirling of the journal in the bearing bushing. The bearing journal becomes unstable as the journal axis begins to perform a circular motion that is bounded only by the walls of the bearing bushing. When the speed threshold is exceeded, the axis of the bearing journal starts to circulate, causing the rotor to vibrate. These vibrations are called whirl. A passive way of how to suppress vibrations consists in adjusting the shape of the bearing bushing, such as lemon or elliptical bore of the bushing, or the use of tilting pads. Even though there are several solutions based on mentioned passive improvements, this article deals with the use of active vibration control (AVC) with piezo-actuators as a measure to prevent instability.

The disadvantage of bearings of this type is whirl instability, which can cause machine tool vibrations. The following chapter describes the possible operating range of the spindle speed.

2. Operating speed range of plain bearings

Special oil for high-speed spindle bearing of the OL-P03 type was used for testing (VG 10 grade, viscosity μ = 0.027 Pa.s at 20°C). Tests were carried out without preheating the lubricant at a normal temperature. The oil viscosity at ambient temperature in the laboratory corresponded to the oil viscosity at 40°C in industrial bearings. The journal bearing cross-section is shown in **Figure 1**.

The operating conditions of the hydrodynamic bearing are described by the Sommerfeld number [1]:

$$S = (R/c)^2 \mu N/P, \qquad (1)$$

where N is a rotational speed of the rotor in rev/s, μ is a dynamic viscosity in Pa.s, R is a radius of the journal, c is a radial clearance, P is a load per unit of projected bearing area ($2RL$) in N/m^2, where L is a bearing length.
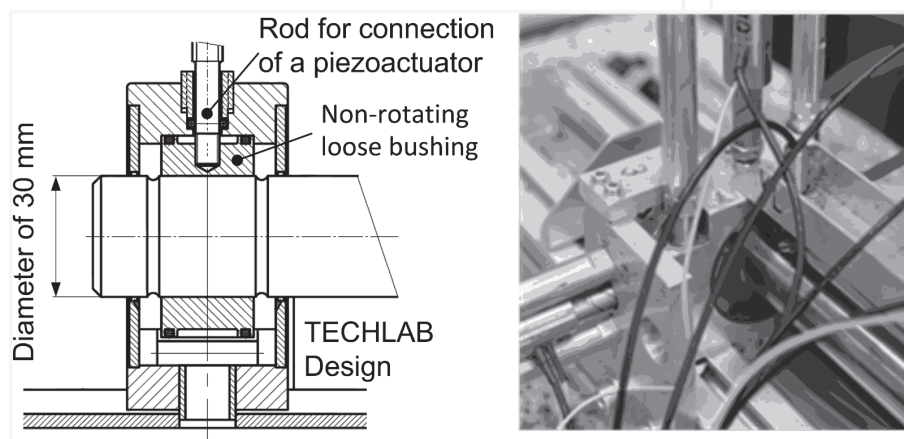

Figure 1.
Side-view technical drawing and a photo of bearing housing.

The value of the Sommerfeld number for the given bearing size and the rotor mass of 0.83 kg is as follows: $R = 0.014 \times N$, where N is the mentioned rotational speed.

The magnitude of friction coefficient in the plain bearings was analysed in the past by the McKee brothers [2]. It has been found that bearing friction is dependent on a dimensionless bearing characteristic given by a ratio $\mu N/P$ whose parameters are defined above. If the rotor does not rotate or rotate slowly, there is only a very thin film between the journal and the bushing. Boundary or thin-film boundary lubrication occurs with a considerably increased coefficient of friction. Many experiments show that the journal axle moves chaotically at low speeds or the journal starts to oscillate. It is uncertain at the start of run-up whether the axle of the bearing journal moves to the left or right, regardless of the direction of rotation. Only when the specified speed limit is exceeded the lubrication becomes hydrodynamic, and thick film of the lubricant is formed, and the trajectory of motion can be predicted. The limit value of the bearing characteristic for the boundary lubrication is described in [1]. Designers keep the value $\mu N/P \geq 1.7 \times 10^{-6}$ (reyn $\times$ rev/s/psi), which is about five times the value the McKee brothers have determined. The measurement in our test rig shows the limit of the boundary lubrication at about 1k rpm, which corresponds to the value of the dimensionless characteristic $\mu N/P$ equaled to 3.8×10^{-5} (Pa.s $\times$ rev/s/Pa) when using SI units for the input parameters. Our estimate for the lower limit of hydrodynamic lubrication corresponds to the recommendations in the handbook [1]. In experiments with the active vibration control, the feedback is closed only for stable lubrication.

An example of a gradual change of position of the bearing journal centre during an increase in speed up to 7k rpm at the constant increase rate is shown in **Figure 2**. The lubrication is of the boundary type in the range up to about 1.2k rpm and is accompanied by oscillations.

The reason for the oscillations is the step change of speed to about 300 rpm after switching on because it is not possible to increase the rotational speed continuously from zero. Hydrodynamic lubrication at stable motion is produced for rotational speed up to 5k rpm. Motion instability of the whirl type occurs when this speed of 5k rpm is exceeded. Fluid force makes sense to be modeled just for stable motion
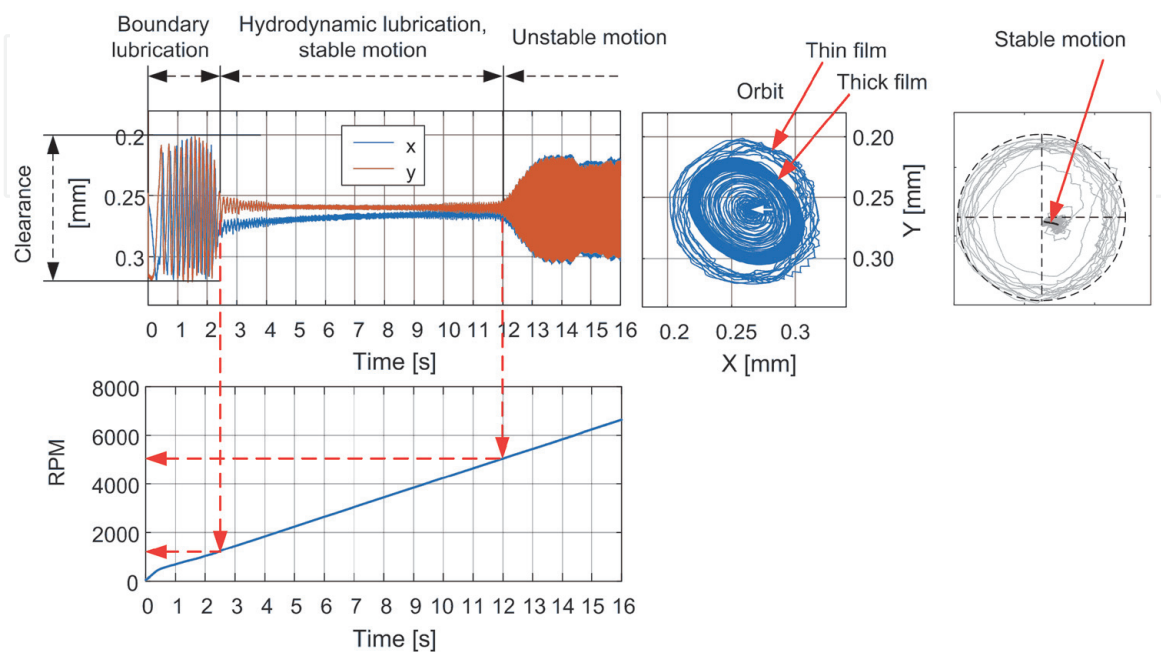

Figure 2.
The run-up of a journal bearing.

and hydrodynamic lubrication. It is almost impossible to determine the initial conditions for boundary lubrication. Notice that the centre of the journal rises to the level of the centre of the bearing bore and gradually approaches this centre so that the small eccentricity gradually decreases to zero as is shown on the right panel of **Figure** 2. The data for this orbit was approximated by the five-degree polynomial in the time interval which begins at the 3rd second and ends at the 12th second. The difference between thin and thick film lubrication is also evident on the right panel of **Figure** 2, which depicts an orbit plot for the entire measurement time up to sixteenth-second.

The threshold of the instability of the journal movement in the bearing is given by the clearance and viscosity of the oil, which depends on the temperature.

3. Instrumentations

For developing a new design of the actively controlled bearing, a test rig was built; see **Figure 3**. This figure provides different views of the test rig. An inductive motor of 400 Hz drives the rotor, and therefore the maximum rotational speed is 23k rpm. The engine is connected to the rotor via the Huco diaphragm coupling. The bearing diameter is 30 mm, and the length-to-diameter ratio is equal to about 0.77. The span of bearing pedestals is of 200 mm. The results of the experiments presented in this article are for the radial clearance of 45 μm. Also, the journals of the other clearance are available for testing. The performance of the actively controlled bearing was tested on the test bench (Rotorkit) of the TECHLAB design [3, 4]. Additionally, it should be emphasised that research was focused at rigid rotors and the journal bushing of the cylindrical bore, where the journal motion is measured at the location closest to the bearing bushing. The research work resulted in putting into operation of the active vibration control system, which became the first functional bearing prototype known up to now [5].

The mechanical arrangement of the actively controlled bearing is shown on the right of **Figure 1**. Oil leakage from the volume between the bearing body and the loose bushing and the piezoactuator rod is sealed with rubber O-rings. As it was stated before, vibrations of the rotor is suppressed using the system for active vibration control with piezoelectric actuators enabling to move the non-rotating loose bushing. The motion of the bearing bushing is controlled by the controller, which responds to the change in position of the bearing journal related to the bearing housing. Two stacked linear piezoactuators are used to actuate the position of the bearing journal via the position of the bearing bushing. The bearing uses a cylindrical bushing which did not require unique technology of production and assembly. This new bearing enables not only to damp vibrations and to prevent
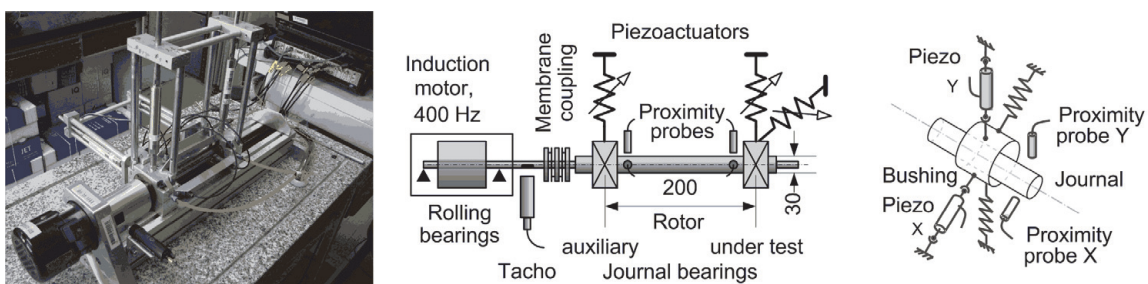

Figure 3.
Actively controlled journal bearings.

instability but also enables to maintain the desired bearing journal position with an accuracy of micrometers.

4. Mathematical model

4.1 Equation of motion

The bearing journal can be considered as a rigid body rotating within the bearing housing at an angular velocity Ω. For simplicity, it is assumed that the rotation axis does not change its direction in contrast to a model [6]. Fluid forces are caused by the hydrodynamic pressure generated in the oil film, whose total mass relative to the journal and rotor is negligible. The oil pumped by the rotating journal surface produces an oil wedge that lifts up the bearing journal so that it does not touch the inner walls of the housing. The coordinate system of a cylindrical journal bearing is shown on the left side in **Figure 4**. The planar motion of the bearing journal at the x and y coordinates can be described by two motion equations arranged into a matrix equation:

$$
\begin{bmatrix} M & 0 \\ 0 & M \end{bmatrix} \begin{bmatrix} \ddot{x} \\ \ddot{y} \end{bmatrix} + \begin{bmatrix} B_{XX} & B_{XY} \\ B_{YX} & B_{YY} \end{bmatrix} \begin{bmatrix} \dot{x} \\ \dot{y} \end{bmatrix} + \begin{bmatrix} C_{XX} & C_{XY} \\ C_{YX} & C_{YY} \end{bmatrix} \begin{bmatrix} x \\ y \end{bmatrix} = \begin{bmatrix} F_X \\ F_Y \end{bmatrix}, \tag{2}
$$

where M is a mass of the rotor; F_X is a force acting on the journal in the horizontal direction; F_Y is a force acting on the journal in the vertical direction; C_{UV} is a stiffness coefficient; and B_{UV} is a damping coefficient, where U is equal to X or Y and V is equal to X or Y as well.

In addition to force components in the horizontal and vertical directions, the force balance will be solved in other possible directions. Force in the direction of the line of the centers is denoted as a direct force F_D, while force which is perpendicular to the line of centers is denoted as a quadrature force F_Q. Both these forces balance the gravity force G, as is shown in the right panel of **Figure 4**.

The system is described by two motion equations, and therefore the total order of the system is four. This system may become unstable even for positive parameter values such as stiffness and damping.
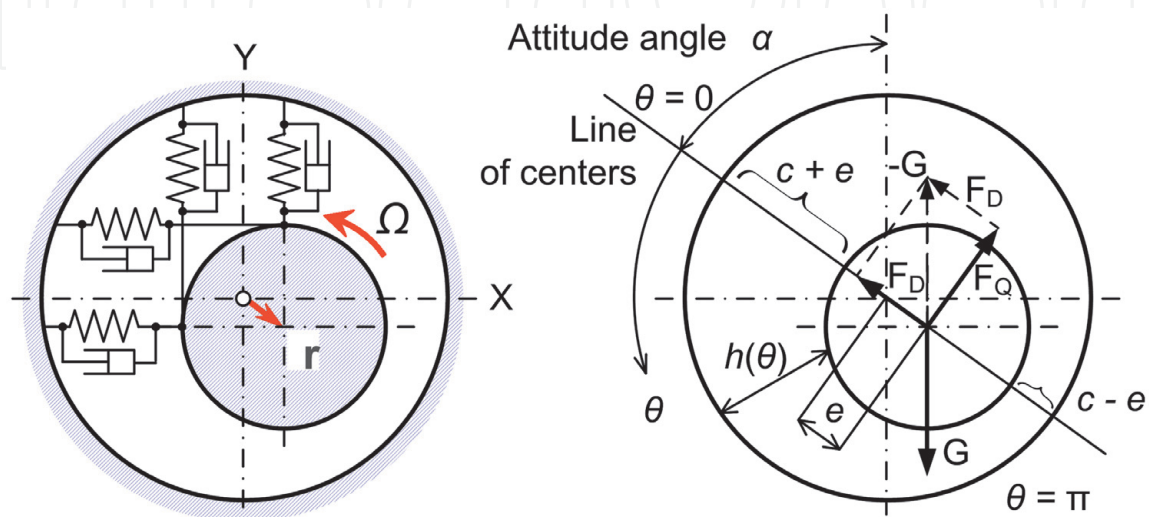

Figure 4.
A cross-section of the hydrodynamic bearing.

4.2 Muszynska model

The motion equation of the rotor with the journal bearing in coordinates x and y was designed by Muszynska. The derivation is based on the design of the formula to calculate the already mentioned direct and quadrature forces. Compared to Eq. (2), the stiffness and damping matrices are designed in such a way that the oil film is replaced by a spring and a dashpot system that rotates at an angular velocity Ω, where λ is a dimensionless parameter, which is slightly less than 0.5. The stiffness of the spring is designated by K, and the damper has a damping factor D:

$$\begin{bmatrix} M & 0 \\ 0 & M \end{bmatrix} \begin{bmatrix} \ddot{x} \\ \ddot{y} \end{bmatrix} + \begin{bmatrix} D & 0 \\ 0 & D \end{bmatrix} \begin{bmatrix} \dot{x} \\ \dot{y} \end{bmatrix} + \begin{bmatrix} K & D\lambda\Omega \\ -D\lambda\Omega & K \end{bmatrix} \begin{bmatrix} x \\ y \end{bmatrix} = \begin{bmatrix} F_X \\ F_Y \end{bmatrix}. \tag{3}$$

The derivation of the motion equation is described, for example, in the article [5].

4.3 Analytical solution of the Reynolds equation

The theory of hydrodynamic bearing is based on a differential equation derived by Osborne Reynolds. Reynolds equation is based on the following assumptions: The lubricant obeys Newton's law of viscosity and is incompressible. The inertia forces of the oil film are negligible. The viscosity μ of the lubricant is constant, and there is a continuous supply of lubricant. The effect of the curvature of the film concerning film thickness is neglected. It is assumed that the film is so thin that the pressure is constant across the film thickness. The shaft and bearing are rigid.

Furthermore, it is assumed that the thickness h of the oil film depends on the other two coordinates, namely, the coordinate z along the axis of rotation and the location on the perimeter of the journal which is described by the angle θ as is shown on the right side in **Figure 4**. If the radius of the bearing journal is equal to R, then the most general version of the Reynolds equation for calculation of the oil pressure distribution $p(\theta, z)$ is as follows (Dwivedy) [7]:

$$\frac{1}{R^2} \frac{\partial}{\partial \theta} \left(h^3 \frac{\partial p}{\partial \theta} \right) + \frac{\partial}{\partial z} \left(h^3 \frac{\partial p}{\partial z} \right) = 6\mu\Omega \frac{\partial h}{\partial \theta} + 12\mu \frac{\partial h}{\partial t}. \tag{4}$$

There is no analytical solution for the Reynolds equation.

During operation, the journal axis shifts from the centre of the bearing bushing to the distance of e, called eccentricity, which is related to a radial clearance c. Variable is called an eccentricity ratio $n = e/c$. The film thickness as a function of θ is defined as follows:

$$h = c(1 + n\cos\theta). \tag{5}$$

The oil film moves in adjacent parallel layers at different speeds, and shear stress results between them. The oil layer at the surface of the journal moves at the peripheral velocity of the journal, while the oil layers at the surface of the bearing bushing do not move (at zero velocity). The surface of the journal moves at a velocity of $U = R\Omega$ in m/s. Reynolds equation will be solved for the steady state and independence of the pressure distribution on the coordinate of z:

$$\frac{d}{d\theta} \left[h^3 \frac{dp}{d\theta} \right] = 6\mu U R \frac{dh}{d\theta}. \tag{6}$$

On double integrating, see [7], we get

$$h^3 \frac{dp}{d\theta} = 6\mu UR \int \frac{dh}{d\theta} d\theta = 6\mu URh + K$$

$$\frac{dp}{d\theta} = 6\mu UR \left[\frac{1}{(1 + n\cos\theta)^2} + \frac{K_1}{c(1 + n\cos\theta)^3} \right] \tag{7}$$

$$p(\theta) = \frac{6\mu UR}{c^2} \int \left[\frac{d\theta}{(1 + n\cos\theta)^2} + \frac{K_1 d\theta}{c(1 + n\cos\theta)^3} \right] + p_0,$$

where $K, K_1,$ and p_0 are integration constants.
The solution must meet the boundary condition:

$$p(\theta = 0) = p(\theta = 2\pi) \Rightarrow p(\theta = 0) - p(\theta = 2\pi) = 0, \tag{8}$$

which gives

$$\frac{6\mu UR}{c^2} \int\limits_{\theta=0}^{\theta=2\pi} \left[\frac{1}{(1 + n\cos\theta)^2} + \frac{K_1}{c(1 + n\cos\theta)^3} \right] d\theta = 0$$

$$\Rightarrow \frac{K_1}{c} = -\frac{\int_{\theta=0}^{\theta=2\pi} 1/\left((1 + n\cos\theta)^2\right) d\theta}{\int_{\theta=0}^{\theta=2\pi} 1/\left(c(1 + n\cos\theta)^3\right) d\theta}. \tag{9}$$

On simplifying, we get a formula for calculating the first integration constant K_1:

$$K_1 = 2c\left(n^2 - 1\right)/\left(n^2 + 2\right). \tag{10}$$

Extreme oil pressure values as a function of the attitude angle θ are achieved if $dp/d\theta = 0$:

$$K_1 = -h = -c(1 + n\cos\theta). \tag{11}$$

The first integration constant is related to the thickness of the oil film at the perimeter of the journal, where the maximum and minimum oil pressure is achieved:

$$h_m = (h)_{p=min} = (h)_{p=max} = -K_1 = \frac{2c(1 - n^2)}{(n^2 + 2)}. \tag{12}$$

The attitude angle where the maximum and minimum pressure occur is given by

$$\cos\theta_m = -3n/\left(n^2 + 2\right). \tag{13}$$

The result of double integration is as follows:

$$p(\theta) = \frac{6\mu UR}{c^2} \frac{n(2 + n\cos\theta)\sin\theta}{(n^2 + 2)(1 + n\cos\theta)^2} + p_0 = \frac{6\mu UR}{c^2} \beta(\theta, n) + p_0. \tag{14}$$

The first integration constant was selected to meet the boundary condition $p_0(0) = p_0(2\pi)$ as is described by Dwivedy et al. The oil pressure distribution on the journal for $n = 0, 0.1, 0.2, \cdots, 0.9$ is shown in **Figure 5**. It should be noticed that the
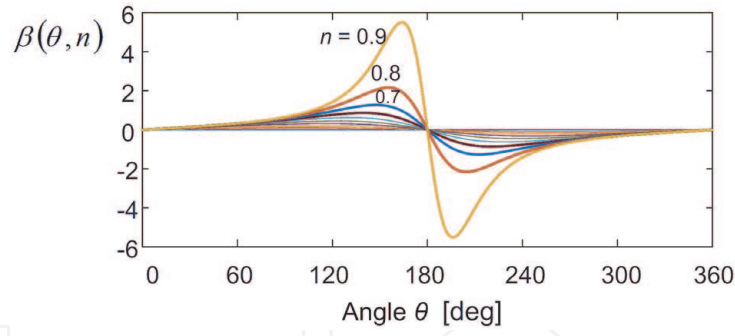
Figure 5.
Pressure distribution along the angular coordinate.

second integration constant has not any effect on the force excited by the oil pressure. The subatmospheric pressure creates a condition for the formation of the cavitation zones.

4.4 Fluid force

The forces acting on the journal in the centre of gravity along the bearing length of L can be calculated for the direction of the line of the centres and the perpendicular direction. Force in the direction of the line of centres is denoted as a direct force F_D, while force which is perpendicular to the line of centres is denoted as a quadrature force F_Q. Both these forces balance the gravity force G as is shown in **Figure 4**:

$$
\begin{aligned}
F_D &= \int_0^{2\pi} p_\theta \cos{(\pi - \theta)} LR \, \mathrm{d}\theta = \\
&= F_N \int_0^{2\pi} \beta(\theta, n) \cos{(\pi - \theta)} \, \mathrm{d}\theta = F_N \beta_D(n) \\
F_Q &= \int_0^{2\pi} p_\theta \sin{(\pi - \theta)} LR \, \mathrm{d}\theta = \\
&= F_N \int_0^{2\pi} \beta(\theta, n) \sin{(\pi - \theta)} \, \mathrm{d}\theta = F_N \beta_Q(n),
\end{aligned}
\tag{15}
$$

where the force F_N can be designated as a nominal force because it corresponds to the maximum force according to the linear model ($n = 1$):

$$
F_N = 6\mu U R^2 L / c^2.
\tag{16}
$$

Note that according to Eq. (14) the pressure on the part of the journal surface is negative, which is, in fact, a relative negative pressure. Since the pressure distribution is antisymmetric with respect to $\theta = \pi$, without evidence, it is clear that these formulas can be applied. Only quadrature force $F_Q > 0$ acts on the bearing journal, and the direct force are zero $F_D = 0$, as is shown on the left panel in **Figure 6**.

The nominal force that multiplies the dimensionless functions $\beta_D(n)$ and $\beta_Q(n)$ can be calculated with the use of the dimensionless Sommerfeld number S and the load P per unit of projected bearing area as follows:

$$
F_N = 6\mu U R^2 L / c^2 = 6\pi S G,
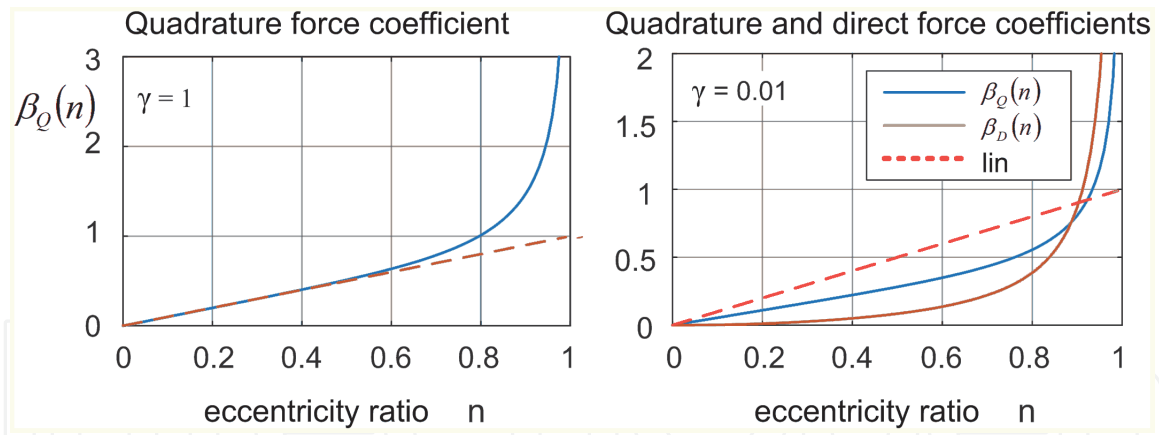\tag{17}
$$

where G is a gravity force.

Figure 6.
Dependence of the direct and quadrature force on the eccentricity ratio.

For speeds ranging from 1.25k to 5k rpm, the force factor F_N varies from 0.46 to 1.8 kN. However, this force is reduced by multiplying the coefficients $\beta_D(n)$ and $\beta_Q(n)$, which depend on the eccentricity ratio n ranging from 0 to 0.33 (0.02/0.06). This case can only theoretically arise in an entirely flooded plain bearing with a vertical axis. The balance of forces F_D, F_Q, and F_Q allows to calculate an attitude angle α:

$$\alpha = \arctan\left(\beta_D(n)/\beta_Q(n)\right). \tag{18}$$

The presence of direct force can be explained, e.g., by the cavitation or the inability to achieve high vacuum, but the mathematical model is more complicated (Ferfecki) [8]. The lubricant flows through the bearing, but in the part of the bearing journal circumference where the pressure is below the barometric pressure, the lubricant can also be sucked. The magnitude of the negative pressure for $\pi < \theta < 2\pi$ is multiplied by a factor γ. Therefore the total force is given by the sum of integrals (Eq. (15)) as follows:

$$\begin{bmatrix} F_D \\ F_Q \end{bmatrix} = \int_0^\pi (\dots)\mathrm{d}\theta + \gamma \int_\pi^{2\pi} (\dots)\mathrm{d}\theta, \tag{19}$$

The effect of negative pressure reduction is demonstrated in the right panel of **Figure 6**. Negative pressure is limited to 1% of the magnitude of positive pressure for the angle interval of $0 < \theta < \pi$. The formulas for the calculation of the quadrature and direct forces contain the same factor $F_N = 6\mu U R^2 L/c^2$ and hence the dependence on the peripheral speed U and therefore on the rotor angular velocity. The coefficients $\beta_Q(n)$ and $\beta_D(n)$ differ considerably, in the experiment, the results of which are shown in **Figure 6**. The eccentricity ratio decreases approximately from 0.3 to 0.07 in the operation at the stable bearing position and stable lubrication. The diagrams confirm the linearity of the quadrature and direct force to eccentricity ratio up to 0.6. The $\beta_Q(n)$ and $\beta_D(n)$ coefficients can be approximated in this range as a linear function:

$$\begin{aligned} \beta_Q(n) &\approx qcn = qe \\ \beta_D(n) &\approx dcn = de, \end{aligned} \tag{20}$$

where q determines the quadrature stiffness $C_Q = 6\mu U R^2 L/c^2 \times q$ and d determines the direct stiffness $C_D = 6\mu U R^2 L/c^2 \times d$.

The stiffness in the directions of the Cartesian coordinates x, y and the attitude angle α which is defined in **Figure 5** can be obtained by substitution:

$$\begin{aligned} x(t) &= -e \sin \alpha \\ y(t) &= +\text{e} \, \cos \alpha. \end{aligned} \tag{21}$$

The vector of the direct and quadrature forces depends on the coordinates x, y according to the following formula:

$$\begin{bmatrix} -C_D e \sin \alpha + C_Q e \cos \alpha \\ C_Q e \sin \alpha + C_D e \cos \alpha \end{bmatrix} = \begin{bmatrix} C_D x + C_Q y \\ -C_Q x + C_D y \end{bmatrix} = \begin{bmatrix} C_D & C_Q \\ -C_Q & C_D \end{bmatrix} \begin{bmatrix} x \\ y \end{bmatrix}. \tag{22}$$

The cross-coupled stiffness $D\lambda\Omega$ according to the Muszynska model corresponds to the expression $6\mu U R^2 L/c^2 \times q$. The direct stiffness K is orderly less than the cross-coupled stiffness; however, the analytical calculation of the stiffness matrix shows the dependence on the rotational speed.

The damping matrix can be derived based on its relationship to the stiffness matrix according to the model that was designed by Muszynska:

$$\begin{bmatrix} D & 0 \\ 0 & D \end{bmatrix} \begin{bmatrix} \dot{x} \\ \dot{y} \end{bmatrix} = \begin{bmatrix} C_Q/\lambda\Omega & 0 \\ 0 & C_Q/\lambda\Omega \end{bmatrix} \begin{bmatrix} \dot{x} \\ \dot{y} \end{bmatrix}. \tag{23}$$

As is $D = C_Q/\lambda\Omega$, the damping coefficient D is a constant. The motion equation for the rigid rotor in the plain bearing is as follows:

$$\begin{bmatrix} M & 0 \\ 0 & M \end{bmatrix} \begin{bmatrix} \ddot{x} \\ \ddot{y} \end{bmatrix} + \begin{bmatrix} C_Q/\lambda\Omega & 0 \\ 0 & C_Q/\lambda\Omega \end{bmatrix} \begin{bmatrix} \dot{x} \\ \dot{y} \end{bmatrix} + \begin{bmatrix} C_D & C_Q \\ -C_Q & C_D \end{bmatrix} \begin{bmatrix} x \\ y \end{bmatrix} = \begin{bmatrix} F_X \\ F_Y \end{bmatrix}. \tag{24}$$

The sum of direct and quadrature forces must compensate for the gravitational force that does not depend on the speed of rotation. The suitability of this model is confirmed by Mendes [9].

If the attitude angle approaches the angle of $\pi/2$ in the radians, then the gravitational force is balanced only by the quadrature force. This state represents the stability limit. The experiment described in this article demonstrates the fact that hydrodynamic lubrication occurs when the eccentricity ratio n is decreased to below the value of 0.33, which happens after a certain speed margin has been exceeded. Unstable lubrication occurs during low revolutions when the eccentricity ratio is higher than the mentioned boundary. The problem of modelling the motion of the bearing journal at low rotational speeds raises the impossibility of determining the initial conditions.

5. Linear time-invariant mathematical model

The coordinate system in the complex plane for the bearing journal position is shown in **Figure 7**. A variable u is a control variable, and a variable r is a controlled variable. The controlled variable is a two-component coordinate of the bearing journal axis, while the control variable is a two-component coordinates of the bushing axis as is shown in **Figure 4**. Because both the variables indicate coordinates in the plane, then they can be considered as two-component vectors. The same meaning as the vector has a complex variables. The real part of this variable has the meaning of the x coordinate, while the imaginary part has the meaning of
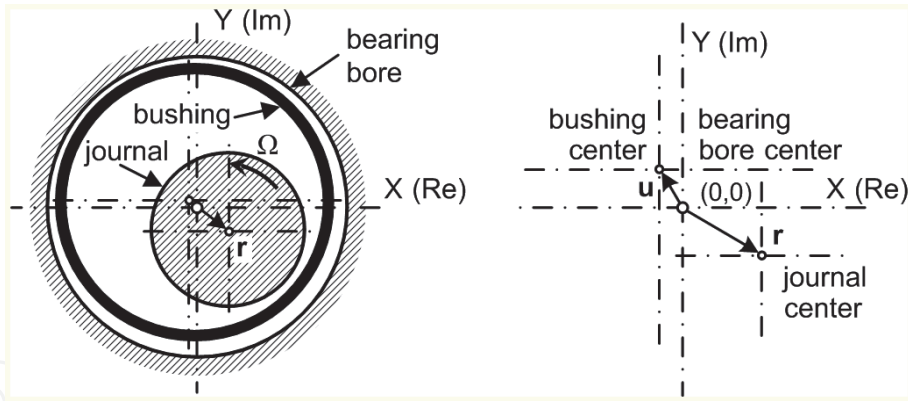
Figure 7.
Coordinate system in the complex plane.

the y coordinate, therefore it is possible to denote it as r = x + jy. The origin (0, 0) of the coordinate system in the complex plane is situated in the center of the mentioned cylindrical bearing bore.

There are many ways how to model journal bearings, but this paper prefers a lumped parameter model, which is based on the concept developed by Muszynska [10]. This concept assumes that the oil film acts as a combination of the spring and damper, which rotates at an angular speed $\lambda\Omega$ (variables will be defined hereinafter). The reason for using this concept was that it offers an effective way to understand the rotor instability problem and to create a model of a journal vibration active control by manipulating the bushing position with the use of actuators, which are a part of the closed-loop system composed of the proximity probes and the controller. If the bearing bushing is stationary ($u = 0$), then the equation of motion at the stationary rotation angular velocity is as follows:

$$M\ddot{r} + D\dot{r} + (K - jD\lambda\Omega)r = F_P \tag{25}$$

where M is the total rotor mass, Ω is the rotor angular velocity, K and D are specifying proportionality of stiffness and damping to the relative position of the journal center displacement vector, λ is a dimensionless parameter which is slightly less than 0.5, and F_P is an oscillating disturbing force defined by ΔF_P exp $(j(\omega t + \varphi_0))$, where ω is a synchronous or nonsynchronous excitation frequency and φ_0 is an initial phase. Excitation frequency is $\omega = 0$ for a static force and $\omega = \Omega$ for imbalance.

Force action of the oil film on the bearing journal can be modeled by Reynolds partial differential equations. The good accuracy of the Muszynska approximate model confirms Mendes and Cavalca [9]. Eq. (2) can be rewritten in matrix form

$$\begin{bmatrix} M & 0 \\ 0 & M \end{bmatrix} \begin{bmatrix} \ddot{x}(t) \\ \ddot{y}(t) \end{bmatrix} + \begin{bmatrix} D & 0 \\ 0 & D \end{bmatrix} \begin{bmatrix} \dot{x}(t) \\ \dot{y}(t) \end{bmatrix} + \begin{bmatrix} K & D\lambda\Omega \\ -D\lambda\Omega & K \end{bmatrix} \begin{bmatrix} x(t) \\ y(t) \end{bmatrix} = \begin{bmatrix} F_x(t) \\ F_y(t) \end{bmatrix}. \tag{26}$$

The entries of the stiffness and damping matrices according to Muszynska model and the calculation of these matrix entries using Reynolds equation agree except for very low rotor speed. Some entries are constants, and others are linear function of the rotational speed. Even entries of the damping matrix are similar. Coordinates of the bearing journal axis for the force of gravity $\boldsymbol{F}_P = 0 - jMg$ is given by the formula:

$$r_0 = Mg \frac{D\lambda\Omega - jK}{(D\lambda\Omega)^2 + K^2} \tag{27}$$

where g is gravitational acceleration. Stiffness of the oil film for static force increases proportionally with rotational speed of the bearing journal:

$$\frac{Mg}{r_0} = D\lambda\Omega + jK. \tag{28}$$

Movement of the bearing journal inside the bearing bushing may be unstable as is apparent from Eq. (26). This phenomenon is called a whirl. The threshold of stability in angular velocity of the rotor can be calculated by the Muszynska's formula:

$$\Omega_{CRIT} = \sqrt{K/M}/\lambda. \tag{29}$$

The equation of motion in the complex form for the rigid rotor operating in a small, localised region in the journal bearing with the movable bushing ($\boldsymbol{u} \neq 0$) is as follows (Eq. (26)):

$$M\ddot{\boldsymbol{r}} + D(\dot{\boldsymbol{r}} - \dot{\boldsymbol{u}}) + (K - jD\lambda\Omega)(\boldsymbol{r} - \boldsymbol{u}) = \boldsymbol{F}_P. \tag{30}$$

The Laplace transform specifies the transfer functions relating the displacement of the bushing to the displacement of the shaft $G_S(s)$, and the disturbance force to the displacement of the shaft $G_F(s)$ are given by

$$\boldsymbol{r}(s) = G_S(s)\boldsymbol{u}(s) + G_F(s)F_P(s), \tag{31}$$

where the mentioned transfer functions are as follows:

$$G_S(s) = \frac{\Delta\boldsymbol{r}(s)}{\Delta\boldsymbol{u}(s)} = \frac{Ds + (K - 1D\lambda\Omega)}{Ms^2 + Ds + (K - jD\lambda\Omega)} \tag{32}$$

$$G_F(s) = \frac{\Delta\boldsymbol{r}(s)}{\Delta\boldsymbol{F}_P(s)} = \frac{1}{Ms^2 + Ds + (K - jD\lambda\Omega)} \tag{33}$$

The active vibration control of journal bearings uses the bushing position as the control variable $\boldsymbol{u}$ and the shaft position as a controlled variable $\boldsymbol{r}$. The control variable is an output of a controller. The controller transforms an error signal computed as a difference of a reference (SP set point) and actual position of the journal. As is evident from the block diagram in **Figure 8**, the controller is of the proportional type with the gain of K_P.

Substituting $s = j\omega$ we can obtain frequency responses of the journal bearing system to harmonic oscillation of the bearing bushing position and disturbance force at the angular frequency $\omega = 2\pi f$ which can differ from the angular velocity Ω. Milling tool excites the strength of a frequency that is an integer multiple of the
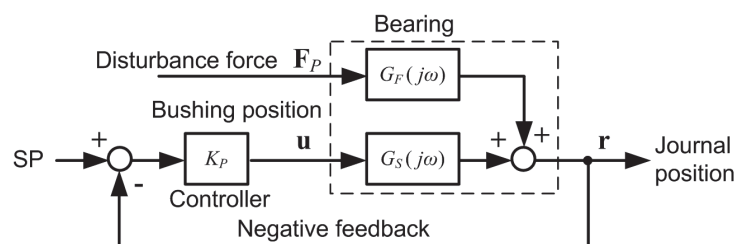

Figure 8.
Closed control loop.

frequency of rotation. The stead-state gain of $G_S(s)$ is equal to unit $G_S(j0) = 1$, while the stead-state gain of $G_F(s)$ depends on the rotor angular velocity as it results from the formula $G_F(j0) = 1/(K - jD\lambda\Omega)$. The reciprocal value of $G_F(j0)$ can be considered as the static stiffness of the oil film without influence of the active vibration control. Stiffness which is defined as a complex value determines the direction of journal axis displacement relative to the direction of the force. The radial force has theoretically identical direction with the journal displacement only at zero speed bearing journal.

The transfer functions relating the set point of the closed-loop system to the displacement of the shaft $G_w(s)$ and the disturbance force to the displacement of the shaft $G_D(s)$ are given by

$$G_w(s) = \frac{K_P G_S(s)}{1 + K_P G_S(s)} = \frac{K_P(Ds + (K - 1D\lambda\Omega))}{Ms^2 + (1 + K_P)Ds + (1 + K_P)(K - jD\lambda\Omega)}, \tag{34}$$

$$G_D(s) = \frac{G_F(s)}{1 + K_P G_S(s)} = \frac{1}{Ms^2 + (1 + K_P)Ds + (1 + K_P)(K - jD\lambda\Omega)}. \tag{35}$$

The stability margin can be calculated under assumption that the open-loop frequency transfer function $G_0(s) = K_P G_S(s)$ of the control loop in **Figure 8** is equal to -1. The frequency of the steady-state vibration at the stability margin is given by $\omega = \lambda\Omega$ and $K_P = \omega^2 M/K - 1$. If the feedback gain K_P is positive, then the maximal rotational speed Ω_{MAX} for the rotor stable behaviour is as follows:

$$\Omega_{MAX} = \Omega_{CRIT}\sqrt{K_P + 1}. \tag{36}$$

If the proportional controller is disconnected, i.e. $K_P = 0$, then the critical angular velocity Ω_{MAX} coincides with the critical frequency Ω_{CRIT} of the closed loop. Increasing of the stability margin for the rotational speed of the rotor is possible by introducing an additional feedback.

The reciprocal value of the transfer function (Eq. (35)) has the meaning of dynamic stiffness for radial force acting at the rotor:

$$C_D(s) = \frac{1}{G_D(s)} = Ms^2 + (1 + K_P)Ds + (1 + K_P)(K - jD\lambda\Omega). \tag{37}$$

If a static force is applied to a rotating journal, then the stiffness of the journal bearing is given by

$$C_D(j0) = \frac{1}{G_D(j0)} = (1 + K_P)(K - jD\lambda\Omega) \tag{38}$$

which means that the stiffness is $(1 + K_P)$ times greater than the journal stiffness without feedback.

Analysis of the effect of active vibration control on the stiffness of the bearing journal assumes a linear mathematical model. Practical calculation of matrix entries of stiffness **C** and damping **B** matrices

$$\mathbf{C} = \begin{bmatrix} C_{XX} & C_{XY} \\ C_{YX} & C_{YY} \end{bmatrix}, \mathbf{B} = \begin{bmatrix} B_{XX} & B_{XY} \\ B_{YX} & B_{YY} \end{bmatrix} \tag{39}$$

shows that the linear model does not differ substantially. The dependence of the matrix entries for the journal bearing of the test rig on the rotor rpm is given by the
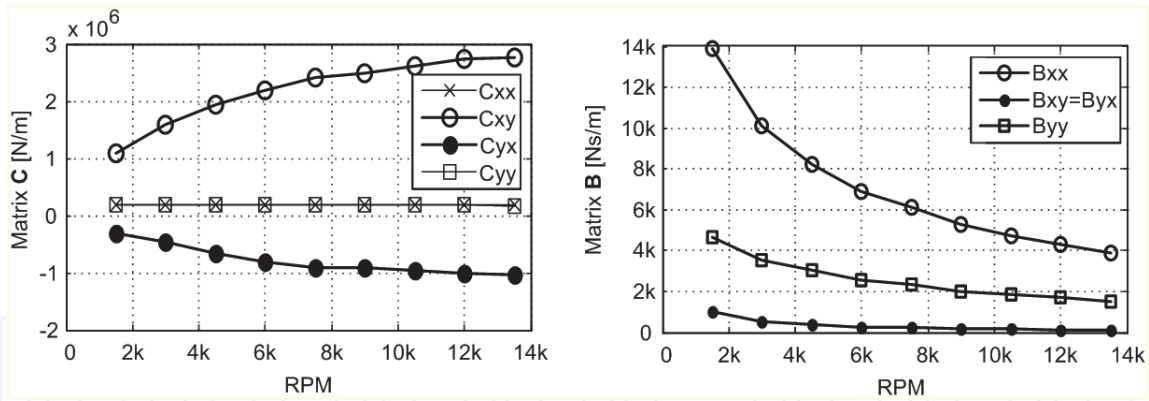
Machine Tools

Figure 9.
Real stiffness and damping matrices according to the Reynolds model.

graphs in **Figure 9**. Pertinent stiffness and damping coefficients are obtained by solving Reynolds equation providing that the journal performs small harmonic motion in neighborhood of its equilibrium position.

6. Limits of the bearing bushing motion

The range of the manipulated variable, which is the position of bearing bushing and at the same time, the controller gain, determines the way to install piezoactuators. The equivalent circuit of the mechanical branch of the control loop for the horizontal direction is shown in **Figure 10**. Parameters that indicate stiffness in the scheme in **Figure 10** are associated to the individual elements of the control loop as follows: K_{PA} is for the piezoactuator, K_S is for the support, and K_{OR} is for the O-ring seal. The piezoactuator is a source of the mechanical travel u_x^* whose
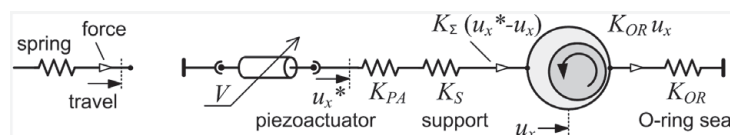
Figure 10.
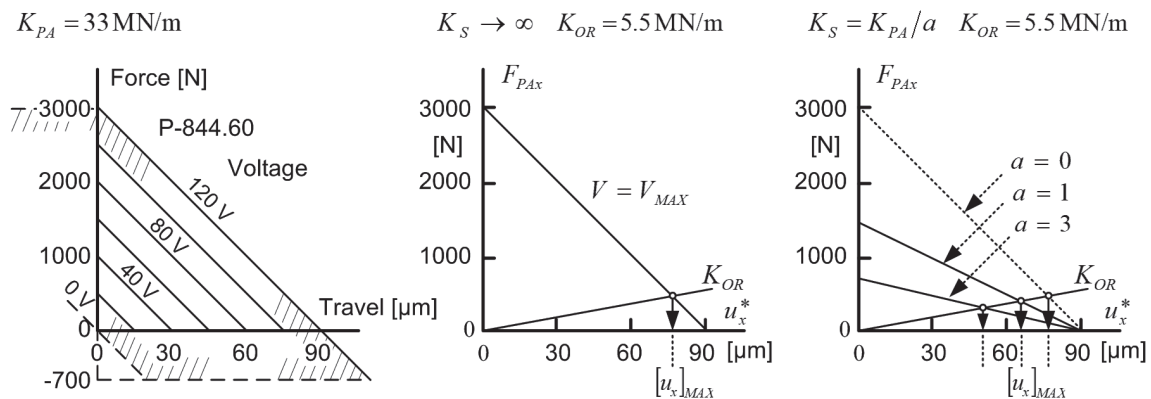*Mechanical branch of the control loop.*

Figure 11.
Piezoactuator operation graphs.

14

magnitude depends on the voltage V. Displacement of the bearing bushing in the horizontal direction is designated as u_x.

The force produced by the piezoactuator balances the force effect of the oil film. Virtual motion of the unloaded piezoactuator is proportional to its control supply voltage $u_x^* = kV$. The resulting motion u_x of the bearing bushing also depends on the load force, as shown in the working graph of **Figure 11**.

Operation graph with all the limitations for the piezoactuator of the P-844.60 type is shown in the left panel of **Figure 11**. If the stiffness of sealing rings is taken into account and the stiffness of the support is assumed to be infinite, then the original range of motion of the bearing bushing is reduced to the size as follows:

$$[u_x]_{MAX} = \frac{[u_x^*]_{MAX}}{1 + K_{OR}/K_{PA}} \tag{40}$$

The effect of the stiffness of the O-ring seal is shown in the middle panel of **Figure 11**. Displacement of the bearing bushing is reduced from 90 to 77 μm for the given parameters of the control loop. The ultimate stiffness of the support affects the virtual stiffness of the piezoactuator as follows:

$$K_{\Sigma} = \frac{K_S K_{PA}}{K_S + K_{PA}} = \frac{K_{PA}}{1 + K_{PA}/K_S} = \frac{K_{PA}}{1 + a} \tag{41}$$

where a is a multiple. Maximum displacement of the bearing bushing respecting all influences is given by the following formula:

$$[u_x]_{MAX} = \frac{[u_x^*]_{MAX}}{1 + (1 + a)K_{OR}/K_{PA}}. \tag{42}$$

First experiments with an imperfect support showed displacement of the bearing bushing of about 20 microns at maximum electrical voltage to supply the piezoactuators. This happened at the beginning of the development when the support arrangement was provisionally extended due to the use of longer piezoactuators. The ideal solution is to install piezoactuators into the bearing housing.

7. Experiments with active control of journal bearings

Experiments with the active vibration control run for several years, while the hardware and software of the control system was upgraded step by step. We have improved design of the piezoactuator support, found suitable sensors for measuring the position of the bearing journal, upgraded the lubrication system, and improved the control algorithm. Properties of the active vibration system have previously been described in the paper [11], and now the main results will be described only, which relate to control the position of the bearing journal.

The instability onset of the bearing journal motion inside the bushing arises when crossing the threshold value of rotational speed Eq. (5). This phenomenon means that the steady-state rotation of the journal is not stable and the journal axis starts to whirl at the frequency, which is 0.42–0.48 multiple of the frequency of rotational speed of the rotor. Measurements in this article were carried out on the shaft with the radial clearance of 45 μm. Rotor speed increases according to a ramp function as it is shown in the left panel of **Figure 12**. The time history of the axis coordinates of the bearing journal is shown in the other panels of **Figure 12**. The x
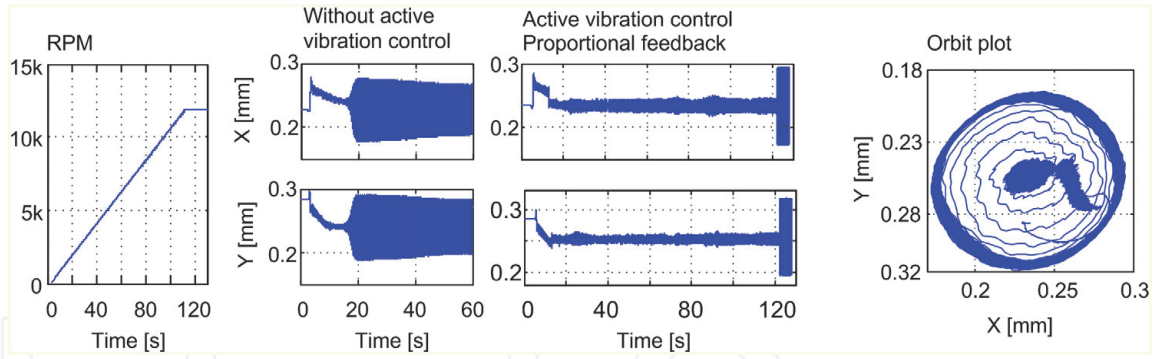
Figure 12.
rpm and the journal position as a function of time.

coordinate corresponds to horizontal direction, and the y coordinate is for vertical direction. Active vibration control is switched off for the time histories in the second panel. Instability occurs at about 2k rpm. This threshold of instability depends on the viscosity of the oil and the bearing clearance. Oscillations of the bearing journal position are limited by the journal clearance within the bushing.

If the active vibration control is switched on and rates of increase of rotational speed are identical for both measurements, the instability of the bearing occurs at the rotational speed about 12k rpm as is shown in the third and fourth panel of **Figure 12** from the left. Vibrations during the instable motion of the journal are also limited by the journal clearance within the inner gap of the bearing bushing.

The transient of the journal seems to be reverse for the vertical motion (y-axis) of the bearing journal in the second and third panel of **Figure 12**. The scale for the vertical motion is reverse in these figures, meaning upside-down. The relationship between horizontal and vertical motion of the journal shows the orbit of the journal axis in the rightmost fourth panel of **Figure 12**. The shape of the orbit is approximately circular when instability occurs.

Threshold of instability is increased six times now using a proportional feedback. According to Eq. (12) this multiple corresponds to the open-loop gain, which is equal to 35. Years ago, we achieved an increase in the threshold of instability only about by 70% for a piezoactuator support with insufficient stiffness. Such an increase of the instability threshold corresponds to the open-loop gain equal to 2.

The active vibration control is not turned on at 0 rpm of the rotor but after finishing a transient process, which ends by lifting the journal to approximately the middle position in the vertical direction which takes approximately 15 seconds for the given rate of the increase of speed.

Through the experiment under specific conditions, the observed onset of instability was at 8450 rpm for control only in the x-axis direction and at 7100 rpm for control only in the y-axis direction [15]. It confirms the rule that static load delays the onset of instability at higher speeds. Control in both directions is required if the direction of the radial force may change or if the rotor has a vertical axis, i.e., the radial force is missing.

The linear proportional controller was used for active vibration control for measurements presented in **Figure 13**. Parametric excitation means that at least one parameter of the system varies periodically in time according to a sinusoidal function, as was suggested by Tondl and Dohnal [12, 13]. The gain of the proportional controller was selected as this varying parameter. The system becomes nonlinear and nonstationary. The gain of the proportional controller is given as follows:

$$K_P = K_{P0}(1 + \alpha \, \sin(\omega_0 t)), \tag{43}$$

where α is dimensionless amplitude of excitation, K_{P0} is static gain factor, and ω_0 is angular frequency of excitation.
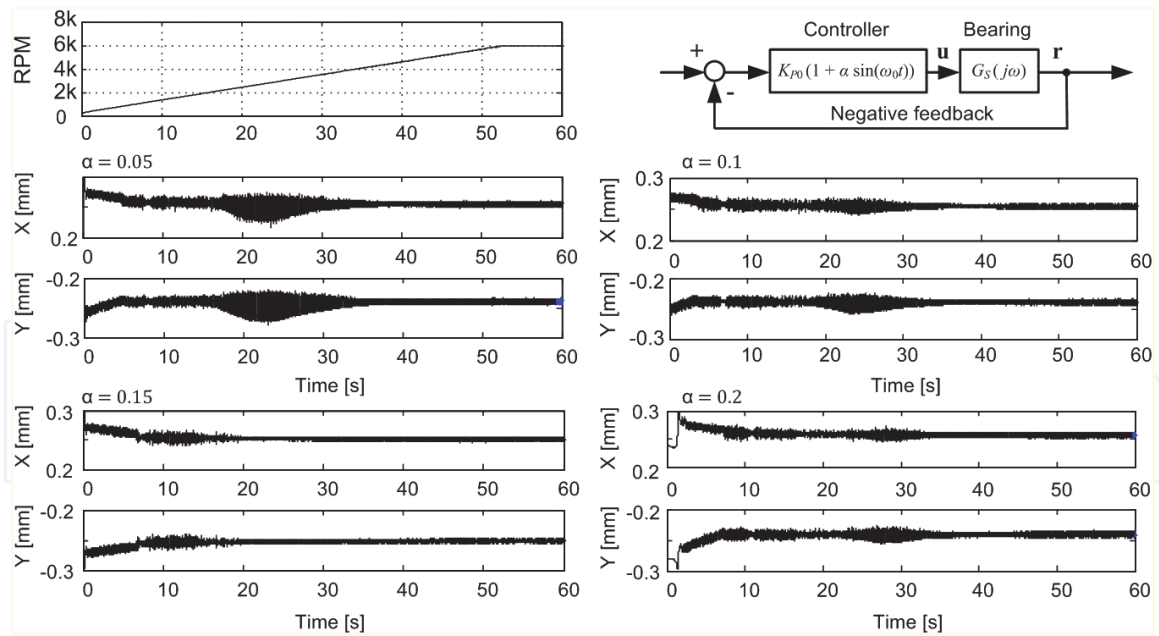
Figure 13.
The journal position as a function of time for tests with active vibration control on.

Dohnal [13] has solved a similar problem for magnetic bearings. Our experiments on the test bench were conducted for the following amplitudes of excitation α = 0, 0.1, 0.15, and 0.2. The static gain was the same as the gain of the previous experiments with the linear controller. The excitation frequency was selected 30 Hz, which is approximately equal to the frequency of vibration at the low rpm. Rotor speed increases according to a ramp function as is shown in the first left panel of **Figure 13**. The effect of the amplitude of the parametric excitation on the journal movement during rotational velocity run-up is shown in other panels of **Figure 13** [11]. The best choice of the excitation amplitude is α = 0.15, which is the position of the journal almost without oscillations. The amplitude of the residual oscillation of the journal does not exceed 8 μm. Precision ball bearings (so-called deep groove ball bearings) which are offered by SKF have a radial clearance (radial internal clearance C2) to a diameter of 30 mm in the range from 1 to 11 micrometers. The maximum rotational speed of the 206-SFFC bearing type is only 7.5k to 13k rpm.

8. Reducing mechanical power losses in actively controlled bearings

Power losses in the journal bearings were estimated from the electric power which is consumed by frequency convertor and motor. Dependence of electrical power upon rotational speed of the motor was measured with and without active control as it is shown in **Figure 14**. Basic power consumption of the motor and
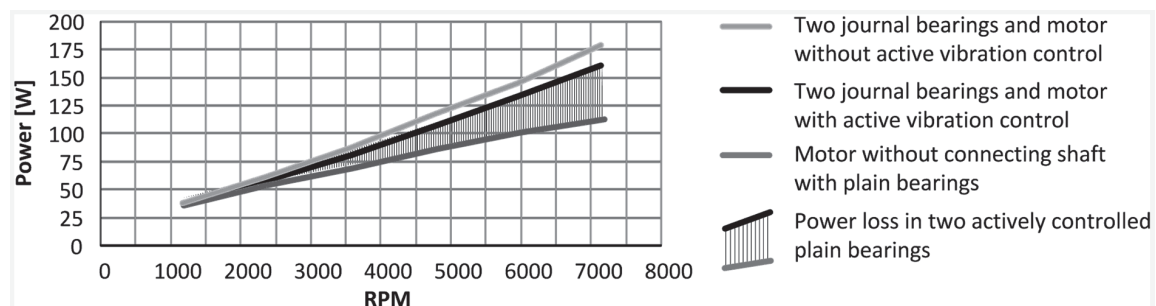

Figure 14.
The electric power consumed by the frequency converter, motor, and bearings.

frequency convertor was measured with the disconnected clutch between the motor and rotor; it means that the bearings were inoperative. The friction loss of a pair of bearings at 7k rpm is 66 W in an unstable operation, and if the active vibration control is on, then the friction loss is of only 48 W. The active vibration control reduces the friction losses of journal bearings by 27%. The bearing clearance amounts to 90 μm for the bearing journal of the diameter 30 mm. As a lubricant the hydraulic oil of the OL-P03 type (VG 10 grade, kinematic viscosity 2.5 to 4 mm^2/s at 40°C) was used. All tests were undertaken at ambient temperature about 20°C. For small power loss by friction in the bearings, the actively controlled bearings can be used in systems for storing the kinetic energy as they are flywheels that spin at high speed. Longer life compared with roller bearings is another advantage of this type of bearings [11].

9. Stiffness of actively controlled bearings

The bearing bushing is suspended on a pair of piezoactuators, and the bearing journal is supported by an oil wedge. According to catalogue data, we used a linear piezoactuator, which is able to generate force of 3 kN in pressure or 700 N in tension on the track in the range of 90 μm. These parameters correspond to the piezoactuator stiffness of 33 MN/m. Stiffness of the force transducer is 2000 MN/m, which is two orders of magnitude higher than the stiffness of piezoactuators. Stiffness of the O-ring seal is 5.5 MN/m which increases the stiffness of the piezoactuator by this value. Force is transmitted to the bearing journal through the oil film. Based on the simulations, it can be estimated that the direct stiffness (C_{XX}) of the oil film in neighborhood of the central position within the bushing bore is of 185 kN/m and the quadrature stiffness (C_{XY} and C_{YX}) is still an order of magnitude larger, and increases proportionally with the rotational speed; see Eq. (39) and **Figure 9**. This stiffness increases by many orders of magnitude if the journal is approaching the bearing bushing wall. Stiffness of the journal support is defined first of all by stiffness of the oil film. A steady-state error in a noncontrolled bearing originates in a radial load which can be considered as a disturbance. A proportional controller which governs a system of journal bearings in the closed-loop with an open-loop gain K_P reduces the steady-state error $(1 + K_P)$ times which results in increase of the oil wedge stiffness $(1 + K_P)$ times compared to the design without a feedback. An integration controller reduces steady-state error to zero, which corresponds to a theoretically infinite stiffness. The use of a derivative component of the controller was also analysed, but additive noise would reduce its effect [14]. Allowable forces, however, are limited by the load capacity of the piezoactuators. The pressure force is thus less than 3 kN. Notice that on the market there are piezoactuators enabling to generate forces up to 20 kN.

Stiffness of precision rolling bearings ranges from 100 to 200 kN/m, regardless of the load, while the stiffness of hydrodynamic bearings in neighborhood of central position (low load) is of the order of several kN/m. However, with active control, the stiffness can increase as much as 35 times, i.e., it can achieve values around 100 kN/m, which is comparable to that of precision ball bearing.

10. Conclusion

Experiments prove the correctness of the theoretical prediction which refers to the extending of the operating range of plain bearings when active vibration control is used. The performance of the actively controlled bearing was tested on the test

rig. The bearing diameter is 30 mm, and the length-to-diameter ratio is equal to about 0.77. The radial clearance of the journal is 45 μm and the very low viscosity oil is used. This combination causes instability of the oil whirl type from the rotational speed of 2k rpm. The active vibration control extends stable operating rotational speed up to 12k rpm, i.e., six times. Also the stiffness of the bearing journal increases significantly during a displacement from equilibrium position. The friction loss of a pair of bearings at 7k rpm is 66 W in an unstable operation, and if the active vibration control is switched ON, then the friction loss is of only 48 W. The active vibration control reduces the friction losses by 27%. The linear proportional controller was used for the active vibration control. The quality of control has been enhanced with the use of periodic changes of the controller gain, which is known as a parametric excitation. The effect of this way of control reduces the journal residual oscillation to the limits which does not exceed 8 μm. This amplitude is comparable with the radial clearance of the ball bearings of the deep groove type. The experiments with the time-periodic changes of the controller gain confirm the positive effect on the vibration response.

Acknowledgements

Author details

Jiří Tůma[1]*, Jiří Šimek[2], Miroslav Mahdal[1], Jaromír Škuta[1], Renata Wagnerová[1] and Stanislav Žiaran[3]

1 Department of Control Systems and Instrumentation, VSB Technical University of Ostrava, Ostrava, Czech Republic

2 TECHLAB Ltd., Prague, Praha, Czech Republic

3 Mechanical Engineering Faculty, The Slovak University of Technology in Bratislava, Slovakia

*Address all correspondence to: jiri.tuma@vsb.cz

IntechOpen

References

[1] Budynas RG, Nisbett JK. Shigley's Mechanical Engineering Design. 9th ed. New York: McGraw-Hill; 2011

[2] McKee SA, McKee TR. Journal bearing friction in the region of thin film lubrication. SAE Journal. 1932;**31**: 371-377

[3] Simek J, Tuma J, Skuta J, Klecka R. Unorthodox behavior of a rigid rotor supported in sliding bearings. In: Proceedings of the Colloquium Dynamics of Machines. Prague: Institute of Thermomechanics; 2010. pp. 85-90

[4] Simek J, Tuma J, Skuta J, Mahdal M. Test stand for affecting rotor behavior by active control of sliding bearings. In: Proceedings of the Colloquium Dynamics of Machines. Prague: Institute of Thermomechanics; 2014. pp. 151-156

[5] Tůma J, Šimek J, Škuta J, Los J. Active vibrations control of journal bearings with the use of piezoactuators. Mechanical Systems and Signal Processing. 2013;**36**:618-629

[6] Wagnerová R, Tůma J. Use of complex signals in modeling of journal bearings. In: 8th Vienna International Conference on Mathematical Modeling. Vienna; Austria: MATHMOD; 2015. pp. 520-525

[7] Dwivedy SK, Tiwari R. Dynamics of Machinery, A Lecture Notes. Guwahati, India: All India Council of Technical Education; 2006

[8] Ferfecki P, Zapomel J. Investigation of vibration mitigation of flexible support rigid rotors equipped with controlled elements. In: 5th International Conference on Modeling of Mechanical and Mechatronic Systems. Vol. 48. Zemplinska Sirava; Slovakia: MMaMS; 2012. pp. 135-142

[9] Mendes RU, Cavalca KJ. On the instability threshold of journal bearing supported rotors. International Journal of Rotating Machinery. 2014;**2014**: 351261

[10] Muszynska A. Whirl and whip – rotor/bearing stability problems. Journal of Sound and Vibration. 1986;**110**(3): 443-462

[11] Tůma J, Šimek J, Mahdal M, Škuta J, Wagnerová R. Actively controlled journal bearings. In: Ecker H, editor. Proceedings of the 12th SIRM Conference. Graz, Österreich; 2017. pp. 443-462

[12] Tondl A. Quenching of Self-Excited Vibrations. Prague: Academia; 1991

[13] Dohnal F, Markert R, Hilsdorf T. Enhancement of external damping of a flexible rotor in active magnetic bearings by time-periodic stiffness. In: Proceedings of the SIRM, Internationale Tagung Schwingungen in rotierenden Maschinen. Darmstadt, Deutschland; 2011

[14] Víteček A, Tůma J, Vítečková M. Stability of rigid rotor in journal bearing. In: Transactions of the VŠB, Mechanical Series. No. 2. Vol. LIV. Technical University of Ostrava; 2008. pp. 159-164

[15] Los J. Mechatronické systémy s piezoaktuátory. VSB Technical University of Ostrava. PhD. Thesis.; 2016